Biochemical insights into Paf1 complex–induced stimulation of Rad6/Bre1-mediated H2B monoubiquitination

Feilong Chen[a,b,1], Beibei Liu[a,b,1], Lu Guo[c], Xuan Ge[d,e], Wei Feng[d,e], De-Feng Li[c,2], Hao Zhou[a,b,2], and Jiafu Long[a,b,2]

[a]State Key Laboratory of Medicinal Chemical Biology, Tianjin Key Laboratory of Protein Science, Nankai University, Tianjin 300071, China; [b]College of Life Sciences, Nankai University, Tianjin 300071, China; [c]State Key Laboratory of Microbial Resources, Institute of Microbiology, Chinese Academy of Sciences, Beijing 100101, China; [d]National Laboratory of Biomacromolecules, Chinese Academy of Sciences Center for Excellence in Biomacromolecules, Institute of Biophysics, Chinese Academy of Sciences, Beijing 100101, China; and [e]College of Life Sciences, University of Chinese Academy of Sciences, Beijing 100049, China

Edited by Robert G. Roeder, The Rockefeller University, New York, NY, and approved July 9, 2021 (received for review December 8, 2020)

The highly conserved multifunctional polymerase-associated factor 1 (Paf1) complex (PAF1C), composed of five core subunits Paf1, Leo1, Ctr9, Cdc73, and Rtf1, participates in all stages of transcription and is required for the Rad6/Bre1-mediated monoubiquitination of histone H2B (H2Bub). However, the molecular mechanisms underlying the contributions of the PAF1C subunits to H2Bub are not fully understood. Here, we report that Ctr9, acting as a hub, interacts with the carboxyl-terminal acidic tail of Rad6, which is required for PAF1C-induced stimulation of H2Bub. Importantly, we found that the Ras-like domain of Cdc73 has the potential to accelerate ubiquitin discharge from Rad6 and thus facilitates H2Bub, a process that might be conserved from yeast to humans. Moreover, we found that Rtf1 HMD stimulates H2Bub, probably through accelerating ubiquitin discharge from Rad6 alone or in cooperation with Cdc73 and Bre1, and that the Paf1/Leo1 heterodimer in PAF1C specifically recognizes the histone H3 tail of nucleosomal substrates, stimulating H2Bub. Collectively, our biochemical results indicate that intact PAF1C is required to efficiently stimulate Rad6/Bre1-mediated H2Bub.

Paf1 complex | H2B monoubiquitination | Rad6/Bre1 | ubiquitin discharge | cooperation

The polymerase-associated factor 1 (Paf1) complex (PAF1C), which was originally identified in *Saccharomyces cerevisiae* as an RNA polymerase II (Pol II)–transcriptional regulator, contains five highly conserved core subunits (Paf1, Leo1, Ctr9, Cdc73, and Rtf1) (1). Human PAF1C includes an additional multifunctional protein, Ski8 (2). An increasing number of studies have demonstrated the conserved role of PAF1C in regulating multiple stages of Pol II transcription, including initiation, protomer-proximal pausing and release, elongation, and RNA processing/termination, in the maintenance of heterochromatin and small RNA-mediated gene silencing or activation (reviewed in ref. 1). Moreover, PAF1C participates in other cellular functions, including DNA repair (3, 4), signal transduction (5), the nuclear export of transcripts (6), cell cycle regulation (7), stem cell pluripotency maintenance (8), autophagy (9), and tumorigenesis (refs. 10–12 and reviewed in refs. 1 and 13). Importantly, most of these functions are mediated, at least in part, by several important histone modifications regulated by PAF1C (14–21).

Ubiquitination of the evolutionarily conserved amino acid lysine 123 in yeast H2B (lysine 120 in humans) is one of the most important histone modifications, which is a prerequisite for specific histone H3 K4 and H3 K79 methylation (di- and tri-) by the Set1 and Dot1 methyltransferases, respectively (22–25), and further establishes acetylation state of active chromatin by recruiting histone acetyltransferase and deacetylase complexes (26–28). Previous studies have shown that H2B ubiquitination is enriched on the regions of active genes (29–31) and that the levels of H2B ubiquitination are correlated with the elongation rates of Pol II (32, 33). Moreover, H2B ubiquitination disrupts local and higher-order chromatin compaction (34), promotes nucleosome reassembly by the FACT histone chaperone complex in vivo (35), and stimulates FACT-dependent chromatin transcription in vitro (36).

In yeast, ubiquitination is catalyzed by the coupling of the ubiquitin-conjugating (E2) enzyme Rad6 with the ubiquitin ligase (E3) Bre1 (human RNF20/40) (37–40). In addition to Rad6 and Bre1, PAF1C is required for the Rad6/Bre1-mediated monoubiquitination of histone H2B K123 (H2Bub) (16, 31, 41, 42). In budding yeast, PAF1C enhances the recruitment of Rad6 and Bre1 to chromatin by binding Bre1, thereby promoting H2Bub (41). Moreover, a previous study showed that PAF1C promotion of H2Bub depends on a histone modification domain (HMD) within the Rtf1 subunit in vivo and that HMD stimulates Bre1-dependent H2Bub by interacting with Rad6 in vitro (31). Expression of the HMD was sufficient to restore global H2Bub in a yeast strain lacking the endogenous *RTF1* gene, the HMD stimulates H2Bub at transcriptionally inactive loci, not preferentially at transcribed genes (42), and the lack of other PAF1C subunits also largely affects H2Bub in yeast (31). These data indicate an important role for intact PAF1C in H2Bub, but the mechanism is still unclear.

Here, we first mapped the Rtf1-binding region on Ctr9 and established a model of yeast *S. cerevisiae* PAF1C assembly. Considering the current knowledge on PAF1C assembly, we further studied the detailed role of each subunit of yeast PAF1C in Rad6/Bre1-mediated H2Bub with a minimal, transcription-free, in vitro ubiquitination

Significance

PAF1C is a highly conserved multiprotein complex composed of five core subunits (Paf1, Leo1, Ctr9, Cdc73, and Rtf1) and is required for Rad6/Bre1-mediated H2B monoubiquitination (H2Bub). This study involves a mechanistic analysis of the contributions of the PAF1C subunits to H2Bub. The results from an established in vitro ubiquitination assay clearly suggest that PAF1C might stimulate H2Bub through multivalent interactions with Rad6 and nucleosomal substrates to facilitate ubiquitin transfer and indicate that intact PAF1C is required to efficiently stimulate Rad6/Bre1-mediated H2Bub.

Author contributions: F.C., H.Z., and J.L. designed research; F.C., B.L., L.G., X.G., W.F., D.-F.L., and H.Z. performed research; F.C., H.Z., and J.L. analyzed data; F.C., H.Z., and J.L. wrote the paper; and J.L. coordinated the research.

The authors declare no competing interest.

This article is a PNAS Direct Submission.

[1]F.C. and B.L. contributed equally to this work.

[2]To whom correspondence may be addressed. Email: jflong@nankai.edu.cn, haozhou@nankai.edu.cn, or lidefeng@im.ac.cn.

This article contains supporting information online at https://www.pnas.org/lookup/suppl/doi:10.1073/pnas.2025291118/-/DCSupplemental.

Published August 12, 2021.

system. Our results revealed that Ctr9 interacts with the eight extreme carboxyl-terminal residues of the Rad6 acidic tail, which is required for PAF1C-induced stimulation of H2Bub. The conserved Cdc73 Ras-like domain can effectively accelerate ubiquitin discharge from Rad6 and thus facilitate H2Bub. Moreover, we found that the Rtf1 HMD promoting H2Bub might be in part through accelerating the Rad6 discharge of ubiquitin and that the Paf1/Leo1 heterodimer specifically recognizes the histone H3 tail of nucleosomal substrates, stimulating Rad6/Bre1-mediated H2Bub.

Results

In Vitro Reconstitution of the Minimal Ctr9/Paf1/Cdc73/Rtf1 Quaternary Complex Derived from Yeast PAF1C. According to prior studies showing that Ctr9 interacts with the N-terminal region of Paf1 and

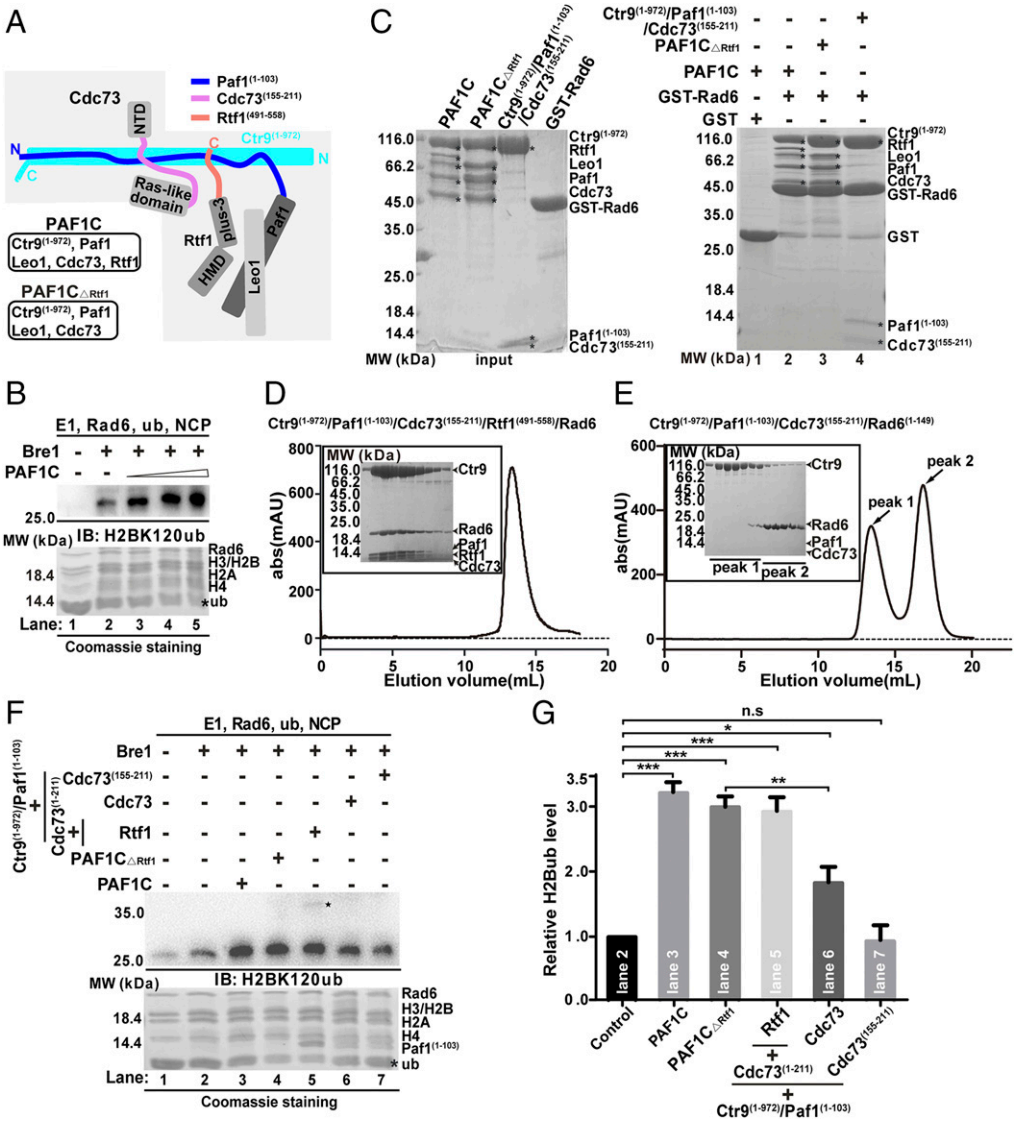

Fig. 1. Rtf1 and Cdc73 are involved in PAF1C-induced stimulation of Rad6/Bre1-mediated H2Bub. (*A*) Yeast PAF1C assembly model. The Ctr9/Paf1 subcomplex functions as a scaffolding heterodimer that binds Cdc73 and Rtf1, and the Leo1 subunit binds PAF1C through the formation of the Paf1/Leo1 heterodimer. The composition of various Paf1 subcomplexes used for biochemical tests is indicated. (*B*) PAF1C stimulated H2Bub in a dose-dependent manner. An in vitro NCP ubiquitination assay was performed in the presence of incremental amounts of PAF1C (lanes 3 through 5 at final concentrations of 1, 2, and 3 μM, respectively). The reactants were incubated for 90 min at 30 °C and analyzed by SDS-PAGE. The top half of the gel was immunoblotted with anti-H2B-K120ub antibody to specifically detect H2B-K120ub, and the bottom half of the gel was stained with Coomassie blue to confirm equal input of the NCPs. The ubiquitin band is marked with an asterisk. (*C*) PAF1C interacts with Rad6 through the Ctr9 subunit. The GST-Rad6 fusion protein was incubated with PAF1C, PAF1C$_{\Delta Rtf1}$, or Ctr9$^{(1-972)}$/Paf1$^{(1-103)}$/Cdc73$^{(155-211)}$ for 1 h at 4 °C. The prepared samples were separated by SDS-PAGE and stained with Coomassie blue (*Right*). Input of the PAF1C and various Paf1 subcomplexes, as indicated, is shown *Left*. (*D* and *E*) The carboxyl-terminal acidic tail of Rad6 is required for the binding of Rad6 to Ctr9. Analytical gel filtration profile and SDS-PAGE of the Ctr9$^{(1-972)}$/Paf1$^{(1-103)}$/Cdc73$^{(155-211)}$/Rtf1$^{(491-558)}$ complex with Rad6 (*D*) or Rad6$^{(1-149)}$ (*E*). The fractions of Ctr9$^{(1-972)}$/Paf1$^{(1-103)}$/Cdc73$^{(155-211)}$ and Rad6$^{(1-149)}$ shown in the corresponding gel are marked as peak 1 and peak 2, respectively. (*F* and *G*) Rtf1 or Cdc73 of PAF1C stimulates Rad6/Bre1-mediated H2Bub. (*F*) An in vitro NCP ubiquitination assay was performed by adding PAF1C or various Paf1 subcomplexes as indicated at a final concentration of 3 μM (lanes 3 through 7). The reactants were incubated for 90 min at 30 °C and analyzed by SDS-PAGE. The top half of the gel was immunoblotted with anti-H2B-K120ub antibody to specifically detect H2B-K120ub, and the bottom half of the gel was stained with Coomassie blue to confirm equal input of the NCPs. The bands representing ubiquitin and diubiquitinated H2B are marked with an asterisk and a star, respectively. (*G*) Quantification of the in vitro NCP ubiquitination assay results shown in *F*. The intensity of the H2Bub band was quantified using ImageJ software. The control (lane 2 in *F*) was used for normalization. The error bars indicate the mean and SD (mean ± SD) (n = 3, separate experiments). n.s, not significant; *P < 0.05; **P < 0.01; ***P < 0.001.

a central region of Cdc73 in thermophilic fungal PAF1C or the human PAF1C assembly (43–45), with sequence alignments of Ctr9 (*SI Appendix*, Fig. S1), Paf1 (*SI Appendix*, Fig. S2*A*), and Cdc73 (*SI Appendix*, Fig. S2*B*) from fungi to humans, we hypothesized that the Ctr9, Paf1, and Cdc73 subunits of yeast PAF1C may form a complex with structural features similar to those of thermophilic fungi and humans. To test this hypothesis, we coexpressed a 972-residue fragment of Ctr9 [amino acids (aa) 1 through 972, $Ctr9^{(1–972)}$], 103-residue fragment of Paf1 [aa 1 through 103, $Paf1^{(1–103)}$], and 57-residue fragment of Cdc73 [aa 155 through 211, $Cdc73^{(155–211)}$] and confirmed that $Ctr9^{(1–972)}$, $Paf1^{(1–103)}$, and $Cdc73^{(155–211)}$ (herein named $Ctr9^{(1–972)}$/$Paf1^{(1–103)}$/$Cdc73^{(155–211)}$, where "/" denotes protein complexes with separate chains and similar structures hereafter) interact by showing the three proteins eluted from a size-exclusion column as a tripartite complex (*SI Appendix*, Fig. S3*A*).

A coimmunoprecipitation assay performed in our previous study showed that yeast Rtf1 can stably associate with PAF1C (46), but this finding was not consistent with Rtf1 weakly interacting with PAF1C in other species (43, 47–49). Combined with the observation that deletion of the Rtf1 carboxyl terminus largely destroyed the interaction between Rtf1 and other components of yeast PAF1C (50), we tested the binding of a 68-residue fragment of Rtf1 [aa 491 through 558, $Rtf1^{(491–558)}$] to the $Ctr9^{(1–972)}$/$Paf1^{(1–103)}$/$Cdc73^{(155–211)}$ complex. Notably, these four proteins assemble into a quaternary complex as indicated by their coelution from an analytical size-exclusion column (*SI Appendix*, Fig. S3*B*). Moreover, we mapped the Rtf1-binding region on Ctr9 using size-exclusion chromatography, and our results indicated that the Rtf1 subunit interacts with the middle region of Ctr9 (aa 313 through 477) (*SI Appendix*, Fig. S3 *C–F*). Collectively, these results showed that the yeast Ctr9/Paf1/Cdc73/Rtf1 subcomplex forms a minimal quaternary complex through interactions between the smallest fragments, $Ctr9^{(1–972)}$ (cyan in Fig. 1*A*), $Paf1^{(1–103)}$ (blue in Fig. 1*A*), $Cdc73^{(155–211)}$ (violet in Fig. 1*A*), and $Rtf1^{(491–558)}$ (salmon in Fig. 1*A*). From these biochemical data and prior studies (43, 45, 46, 49), a model of yeast PAF1C was established (Fig. 1*A*). The Ctr9/Paf1 subcomplex functions as a scaffolding heterodimer that binds Cdc73 and Rtf1, and the Leo1 subunit binds PAF1C through formation of an Leo1/Paf1 heterodimer. All sodium dodecyl sulfate–polyacrylamide gel electrophoresis (SDS-PAGE) gels loaded with the purified subcomplexes, including various tripartite complexes and the quaternary complex, are shown in *SI Appendix*, Fig. S3.

PAF1C Promotes Rad6/Bre1-Mediated H2Bub In Vitro. Although PAF1C is required to promote H2Bub in vivo (16), the biochemical mechanism of PAF1C in Rad6/Bre1-mediated H2Bub is still unclear. To further test the function of each subunit of PAF1C in the process of Rad6/Bre1-mediated H2Bub, we used a minimal, transcription-free in vitro ubiquitination system. Moreover, according to the findings showing that the expression of the $Ctr9^{(1–972)}$ fragment fully reversed the *ctr9Δ* phenotype (*SI Appendix*, Fig. S4*A*) and that $Ctr9^{(1–972)}$ was sufficient to bind Paf1, Cdc73, and Rtf1 (*SI Appendix*, Fig. S3), as well as the finding that full-length Ctr9 was easily degraded during purification, $Ctr9^{(1–972)}$ was used to generate various recombinant Paf1 protein subcomplexes. Accordingly, we purified recombinant holo-PAF1C proteins [$Ctr9^{(1–972)}$, Rtf1, Leo1, Paf1, and Cdc73] (*SI Appendix*, Fig. S4*B*), nucleosomes, and various components of the ubiquitination system (E1 [Uba1], E2 [Rad6] or Myc-tagged Rad6 [Myc-Rad6], E3 [Bre1], and ubiquitin [ub] or Myc-tagged ubiquitin [Myc-ub]) (*SI Appendix*, Fig. S4*C*). Notably, PAF1C directly stimulated Rad6/Bre1-mediated H2Bub in a dose-dependent manner (Fig. 1*B*). Moreover, we noted that the amount of available ubiquitin decreased as the concentration of PAF1C increased (Fig. 1*B*; the position of ubiquitin on the SDS-PAGE gel is marked with an asterisk) and wanted to test the signals of Myc-ub throughout the entire gel to monitor various ubiquitination products. Notably, a large amount of ubiquitin modified Bre1, and a small amount of ubiquitin modified H2B (*SI Appendix*, Fig. S4*D*). Together, these results indicated that PAF1C might accelerate a certain process of ubiquitin transfer to Bre1 or H2B.

A prior study demonstrated that the interaction between the HMD of Rtf1 and Rad6 can be detected in vivo (31). We next used a glutathione S-transferase (GST) pull-down assay to detect the interaction between holo-PAF1C and Rad6. Holo-PAF1C was indeed pulled down by GST-Rad6 (Fig. 1 *C*, *Right*, lane 2). Interestingly, the interaction between Rad6 and the PAF1C lacking Rtf1 (referred to as $PAF1C_{\Delta Rtf1}$, Fig. 1*A*) was not affected (Fig. 1*C*, lane 3), indicating that subunits of PAF1C other than Rtf1 may directly interact with Rad6. The tetratricopeptide repeat (TPR) motif has been reported to constitute interaction surfaces in other proteins (51), and Ctr9 possesses multiple TPR motifs (43, 45), suggesting that Ctr9 might directly bind Rad6. Accordingly, we purified the $Ctr9^{(1–972)}$/$Paf1^{(1–103)}$/$Cdc73^{(155–211)}$ subcomplex [$Paf1^{(1–103)}$ or $Cdc73^{(155–211)}$ was the minimal fragment required to bind Ctr9 and thus did not bind other proteins] to detect the interaction between Ctr9 and Rad6. As anticipated, $Ctr9^{(1–972)}$/$Paf1^{(1–103)}$/$Cdc73^{(155–211)}$ was strongly pulled down by GST-Rad6 in buffer containing 100 mM NaCl (Fig. 1*C*, lane 4). Next, we purified subcomplexes containing several truncated Ctr9 constructs (*SI Appendix*, Fig. S4 *E* and *F*) to further map the Rad6-binding region of Ctr9 using GST pull-down assays and found that residues 764 through 912 of Ctr9 are essential for Rad6 binding (*SI Appendix*, Fig. S4 *E* and *G*).

Moreover, we further tested the interaction between Ctr9 and Rad6 using size-exclusion chromatography. However, Rad6 did not coelute with the $Ctr9^{(1–972)}$/$Paf1^{(1–103)}$/$Cdc73^{(155–211)}$ complex from a size-exclusion column with buffer containing 200 mM NaCl (*SI Appendix*, Fig. S5*A*), indicating that a high salt concentration may affect the interaction between Rad6 and Ctr9. Accordingly, buffers containing different salt concentrations were used to wash the beads used in the GST pull-down assay. We found that Ctr9 was pulled down by GST-Rad6 in a low-salt buffer (100 mM NaCl) but not in buffers with higher salt concentrations (200 to 1,000 mM NaCl) (*SI Appendix*, Fig. S5*B*, lane 1 compared to lanes 2 through 4) and that Rad6 formed a stable complex with the $Ctr9^{(1–972)}$/$Paf1^{(1–103)}$/$Cdc73^{(155–211)}$/$Rtf1^{(491–558)}$ complex in a size-exclusion column under physiological salt conditions (100 mM NaCl) (Fig. 1*D*). These results showing that the interaction between Ctr9 and Rad6 is salt concentration sensitive, together with the observation showing that yeast Rad6 has a carboxyl-terminal acidic tail in contrast to other species (*SI Appendix*, Fig. S5*C*) and previous data showing that the carboxyl-terminal acidic tail is required for normal Rad6-mediated H2Bub levels in yeast (38), suggest that the carboxyl-terminal acidic tail of Rad6 may directly bind Ctr9. Accordingly, the carboxyl-terminal acidic residues (aa 150 through 172) were deleted from Rad6 [referred to as $Rad6^{(1–149)}$] (*SI Appendix*, Fig. S5*C*). As anticipated, mutant $Rad6^{(1–149)}$ did not bind Ctr9 in either the GST pull-down assay (*SI Appendix*, Fig. S5*D*, lane 3) or size-exclusion chromatography (Fig. 1*E*). Additionally, a GST pull-down analysis showed that $Rad6^{(1–149)}$ failed to interact with holo-PAF1C (*SI Appendix*, Fig. S5*E*, lane 3). Notably, the acidic tail is required for the intrinsic ubiquitin-conjugation activity of Rad6 (41). Interestingly, we found that mutant $Rad6^{(1–164)}$ (with the eight extreme carboxyl-terminal residues of Rad6 deleted; *SI Appendix*, Fig. S5*C*) exhibited intrinsic activity similar to that of wild-type Rad6 (*SI Appendix*, Fig. S6*A*, lane 6 compared to lane 2, and *SI Appendix*, Fig. S6*B*) but did not form a stable complex with Ctr9 (*SI Appendix*, Fig. S6*C*). Notably, the efficiency of PAF1C stimulation of H2Bub was decreased in the context of the mutant $Rad6^{(1–164)}$ (*SI Appendix*, Fig. S6*A*, lanes 7 and 8 compared to lanes 3 and 4, and *SI Appendix*, Fig. S6*B*). Collectively, these findings indicated that Ctr9, which directly

interacts with the eight extreme carboxyl-terminal residues of the acidic tail of Rad6, might serve as a platform for other subunits of PAF1C to stimulate Rad6/Bre1-mediated H2Bub.

To test this hypothesis, we prepared holo-PAF1C and various Paf1 subcomplexes PAF1C$_{\Delta Rtf1}$ (lacking Rtf1), Ctr9$^{(1-972)}$/Paf1$^{(1-103)}$/Cdc73$^{(1-211)}$/Rtf1, Ctr9$^{(1-972)}$/Paf1$^{(1-103)}$/Cdc73, and Ctr9$^{(1-972)}$/Paf1$^{(1-103)}$)/Cdc73$^{(155-211)}$ (*SI Appendix*, Fig. S6*D*, lanes 1 through 5, respectively) and tested the ability of these purified complexes to stimulate H2Bub. As anticipated, we observed that both PAF1C and Ctr9$^{(1-972)}$/Paf1$^{(1-103)}$/Cdc73$^{(1-211)}$/Rtf1 stimulated H2Bub (Fig. 1 *F*, *Top*, lanes 3 and 5 compared to lane 2, and Fig. 1*G*). Interestingly, we found that either PAF1C$_{\Delta Rtf1}$ or Ctr9$^{(1-972)}$/Paf1$^{(1-103)}$/Cdc73, but not Ctr9$^{(1-972)}$/Paf1$^{(1-103)}$/Cdc73$^{(155-211)}$, stimulated H2Bub (Fig. 1 *F*, *Top*, lanes 4 and 6 compared to lanes 2 and 7, and Fig. 1*G*), indicating that the Cdc73 subunit (probably via its carboxyl-terminal Ras-like domain, for a detailed study, see next section) has a previously unidentified function in PAF1C-induced Rad6/Bre1-mediated H2Bub.

The Cdc73 Ras-like Domain Accelerates Ubiquitin Discharge from Rad6. Cdc73 contains a conserved carboxyl-terminal Ras-like domain (Fig. 2*A*). The carboxyl-terminal domain of Cdc73 adopts a Ras-GTPase fold that contributes to the recruitment of PAF1C to chromatin and functions in redundant fashion with Rtf1 in the mediation of histone methylation, and deletion of this Ras-like domain led to the acquisition of phenotypes associated with defects in transcription (52). These observations, together with the finding showing that the Cdc73 subunit is involved in PAF1C-induced stimulation of H2Bub (Fig. 1 *F* and *G*), suggested that the conserved Ras-like domain of Cdc73 might play a role in Rad6/Bre1-mediated H2Bub. Accordingly, we prepared the complexes Ctr9$^{(1-972)}$/Paf1$^{(1-103)}$/Cdc73$^{(155-393)}$ (containing the Ras-like domain) and Ctr9$^{(1-972)}$/Paf1$^{(1-103)}$/Cdc73$^{(1-211)}$ (lacking the Ras-like domain) to test the potential role of the Ras-like domain of Cdc73 in stimulating H2Bub (Fig. 2*A* and *SI Appendix*, Fig. S7*A*). Notably, we found that Cdc73$^{(155-393)}$, but not Cdc73$^{(1-211)}$, promoted H2Bub (Fig. 2*B*, lanes 3 and 4 compared to lane 2, and Fig. 2*C*). Additionally, we noted the Rad6-binding

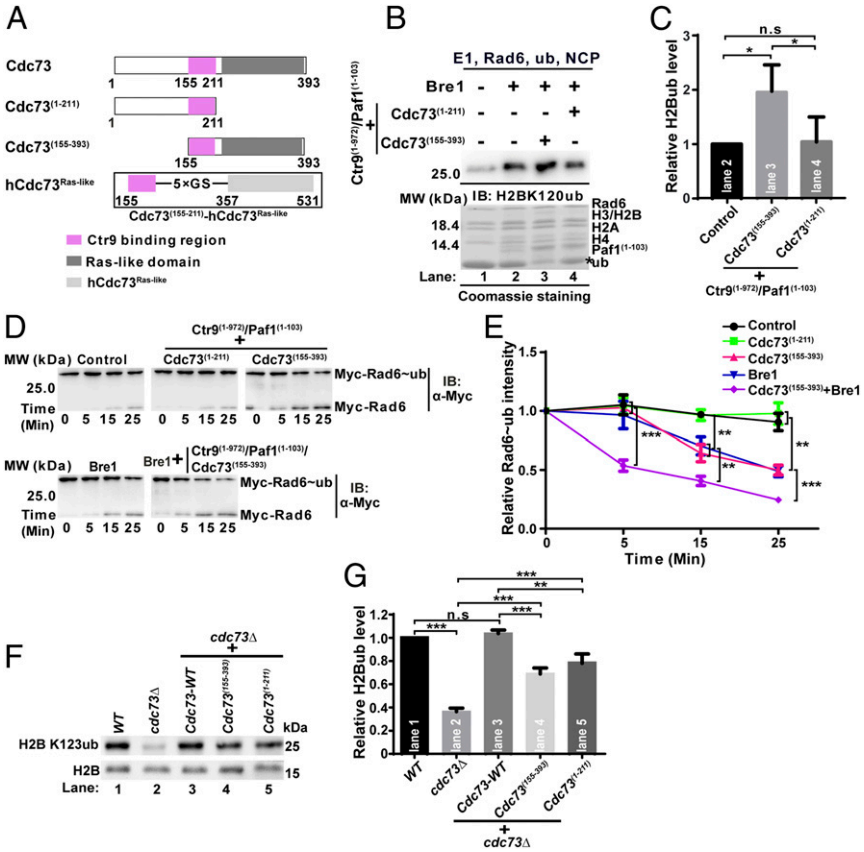

Fig. 2. The Cdc73 Ras-like domain accelerates ubiquitin discharge from Rad6. (*A*) Schematic representation of various fragments of the subunit Cdc73 or the chimera Cdc73$^{(155-211)}$-hCdc73$^{Ras-like}$ that were coexpressed with Ctr9$^{(1-972)}$/Paf1$^{(1-103)}$ is shown. The chimera was designed by fusing yeast Cdc73$^{(155-211)}$ to the N terminus of the human Cdc73 Ras-like domain (hCdc73$^{Ras-like}$). The Ctr9-binding region and Ras-like domain of Cdc73 are colored violet and gray, respectively. (*B* and *C*) The Cdc73 Ras-like domain stimulates H2Bub. (*B*) An in vitro NCP ubiquitination assay was performed by adding the indicated purified complexes. The reactants were incubated for 90 min at 30 °C and analyzed by SDS-PAGE. The top half of the gel was immunoblotted with anti-H2B-K120ub antibody to specifically detect H2B-K120ub, and the bottom half of the gel was stained with Coomassie blue to confirm equal input of the NCPs. The ubiquitin band is marked with an asterisk. (*C*) Quantification of the in vitro NCP ubiquitination assay results shown in *B*. The intensity of the H2Bub band was quantified using ImageJ software. The control (lane 2 in *B*) was used for normalization. (*D* and *E*) The Cdc73 Ras-like domain accelerates ubiquitin discharge from Rad6. (*D*) Representative immunoblot analysis of a single-turnover ubiquitin discharge experiment in which precharged Myc-Rad6~ub was incubated without or with Bre1 and/or various Paf1 subcomplexes as indicated at a final concentration of 3 μM. Aliquots were collected after 0, 5, 15, and 25 min of denaturation. The samples were separated by nonreducing SDS-PAGE followed by anti-Myc immunoblotting. (*E*) Quantification of the results of the turnover experiments in *D*. The intensity of the Myc-Rad6~ub band was quantified using ImageJ software, and the intensity at time 0 was used for normalization. (*F*) The human anti-H2B-K120ub antibody can also specifically detect the H2B-K123ub in yeast (*Top*) or with anti-H2B antibody to confirm equal loading (*Bottom*). (*G*) Quantification of the intensity of H2Bub bands shown in *F*. Three independent experiments were performed for *B* and *D*, and *F*, respectively, and then used for quantification. The error bars in *C*, *E* and *G* indicate the mean and SD (mean ± SD) ($n = 3$, separate experiments). n.s, not significant, $^*P < 0.05$, $^{**}P < 0.01$, $^{***}P < 0.001$.

region of Ctr9 was closed to the Cdc73-binding region of Ctr9 (*SI Appendix*, Fig. S4*E*) and thus speculated that the Cdc73 Ras-like domain might likely bind Rad6. To test this hypothesis, we individually purified Rad6, Cdc73$^{(1-211)}$, and Cdc73$^{(155-393)}$ for a glutaraldehyde cross-linking assay. As anticipated, Cdc73$^{(155-393)}$, but not Cdc73$^{(1-211)}$, and Rad6 could efficiently form cross-linking products with high molecular weights (*SI Appendix*, Fig. S7*B*, lane 10 compared to lane 8). As negative control, Rad6, Cdc73$^{(1-211)}$, or Cdc73$^{(155-393)}$ could not form cross-linking products under the same conditions (*SI Appendix*, Fig. S7*B*, lanes 2, 4, or 6, respectively). These results indicated that the Cdc73 Ras-like domain binds Rad6 directly, and it is conceivable that the binding affinity between Cdc73 and Rad6 might be enhanced by the presence of the scaffold protein Ctr9.

According to prior studies showing that the Bre1-RBD (Rad6-binding domain) interacts with Rad6 and accelerates the discharge of ubiquitin from Rad6 (39, 40), we speculated that the Cdc73 Ras-like domain might also accelerate the catalytic activity of Rad6. Accordingly, we directly analyzed the dissolution of the ubiquitin thioester (~ub) from the active residue of Rad6 near the Cdc73 Ras-like domain or the ubiquitin ligase (E3) Bre1 (as the positive control) in an E2 discharge assay. Notably, we found that Cdc73$^{(155-393)}$ (containing the Ras-like domain) but not Cdc73$^{(1-211)}$ (lacking the Ras-like domain) accelerated the rate of ubiquitin discharge from Rad6 (Fig. 2*D* and the magenta or green line compared to the black line in Fig. 2*E*) and that the discharge efficiency of Cdc73$^{(155-393)}$ is similar to that of Bre1 (Fig. 2*D* and the magenta line compared to the blue line in Fig. 2*E*). Moreover, we found that Cdc73$^{(155-393)}$ and Bre1 simultaneously accelerated the ubiquitin discharge from Rad6 (Fig. 2*D* and the purple line compared to the magenta and blue lines in Fig. 2*E*). To further evaluate the role of the Ras-like domain of Cdc73 in stimulating H2Bub by accelerating E2 discharge, a chimera was designed by fusing yeast Cdc73$^{(155-211)}$ to the human Cdc73 Ras-like domain (hCdc73$^{\text{Ras-like}}$) with a linker (5×GS) [referred to as Cdc73$^{(155-211)}$-hCdc73$^{\text{Ras-like}}$ or hCdc73$^{\text{Ras-like}}$ for convenience] (Fig. 2*A* and *SI Appendix*, Fig. S7*A*, lane 2). Interestingly, the purified Ctr9$^{(1-972)}$/Paf1$^{(1-103)}$)/Cdc73$^{(155-211)}$-hCdc73$^{\text{Ras-like}}$ complex stimulated H2Bub (*SI Appendix*, Fig. S7*C*, lane 5 compared to lane 2, and *SI Appendix*, Fig. S7*D*) by accelerating ubiquitin discharge from Rad6 (hCdc73$^{\text{Ras-like}}$ compared to the control as shown in *SI Appendix*, Fig. S7 *E* and *F*), indicating that the function of the Ras-like domain of Cdc73 in stimulating H2Bub by accelerating E2 discharge of ubiquitin might be evolutionarily conserved. Collectively, these results showed that the Cdc73 Ras-like domain has the potential to accelerate the catalytic activity of Rad6 and thus stimulates H2Bub.

Next, we further investigated the role of Cdc73 in H2Bub in yeast. To this end, a *cdc73Δ* strain was generated by replacing the *CDC73* gene with *S. cerevisiae URA3* (*SI Appendix*, Table S1). Consistent with the previous result (53), the deletion of Cdc73 (*cdc73Δ*) resulted in a drastically reduced level of H2Bub (Fig. 2*F*, lane 2 compared to lane1, and Fig. 2*G*). When expressed in the *cdc73Δ* yeast strain, wild-type Cdc73 (*Cdc73-WT*) fully restored the level of H2Bub (Fig. 2*F*, lane 3 compared to lane 1, and Fig. 2*G*), while Cdc73$^{(155-393)}$ (containing the Ras-like domain) partially restored the level of H2Bub (Fig. 2*F*, lane 4 compared to lanes 2 and 3, and Fig. 2*G*), indicating that the *N*-region of Cdc73 also plays a role in H2Bub. Accordingly, the expression of Cdc73$^{(1-211)}$ in the *cdc73Δ* yeast strain indeed partially restored the level of H2Bub (Fig. 2*F*, lane 5 compared to lanes 2 and 3, and Fig. 2*G*). Together, these results indicated that both the Ras-like domain and the *N*-region of Cdc73 are important for optimal H2Bub in vivo.

The Rtf1 HMD Accelerates Ubiquitin Discharge from Rad6 in a Manner Similar to that of the Cdc73 Ras-like Domain. Rtf1 is a multifunctional subunit of PAF1C (50) with two highly conserved domains, HMD and the plus-3 domain (Fig. 3*A*). The plus-3 domain plays a role in the recruitment of PAF1C by interacting with Spt5 (54), and the HMD is required for PAF1C to promote H2Bub in vivo (14, 50, 55). Deletion or mutation of the HMD can abrogate H2Bub in *S. cerevisiae*, and expression of the HMD is sufficient to restore the global H2Bub levels in Rtf1-deleted yeast (31, 42). Structural data and in vivo site-specific cross-linking revealed that the HMD and Rad6 directly interact (31). These studies provided abundant evidence that the HMD directly promotes H2Bub; however, the molecular mechanism remains unclear.

To determine the role of the HMD and plus-3 domain of Rtf1 in Rad6/Bre1-mediated H2Bub, the full-length Rtf1, Rtf1$^{(241-558)}$ (lacking HMD), or Rtf1$^{(371-558)}$ (lacking both the HMD and plus-3 domain) fragment was copurified with Ctr9$^{(1-972)}$/Paf1$^{(1-103)}$)/Cdc73$^{(155-211)}$ [Cdc73$^{(155-211)}$ lacking the Ras-like domain to prevent Cdc73-induced stimulation of H2Bub] (*SI Appendix*, Fig. S8*A*, lanes 1 through 3). Notably, the level of H2Bub was increased with the addition of full-length Rtf1 but not with Rtf1$^{(241-558)}$ or Rtf1$^{(371-558)}$ (both lacking the HMD) (Fig. 3*B*, lane 3 compared to lanes 4 and 5, and Fig. 3*C*), indicating that, in our assay system, the HMD of Rtf1 plays a very important role in Rad6/Bre1-mediated H2Bub, which is consistent with previous reports (31, 42). Moreover, we introduced a point mutation (E104K) in the HMD (*SI Appendix*, Fig. S8*A*, lane 4), which was shown to abolish the H2Bub in yeast (31) and found that this Rtf1 mutant indeed lost its ability to stimulate H2Bub in the ubiquitination assay (Fig. 3*D*, lane 4 compared to lane 3). Importantly, the E2 discharge assay showed that full-length Rtf1, but not Rtf1$^{(241-558)}$ (lacking the HMD), exhibit an increase in the rate of ubiquitin discharge from Rad6 (Fig. 3*E* and the magenta or green line compared to the black line in Fig. 3*F*) and that the discharge efficiency of Rtf1 is similar to that of Bre1 (positive control) (Fig. 3*E* and the magenta line compared to the blue line in Fig. 3*F*). Additionally, we found that Rtf1 and Bre1 accelerated ubiquitin discharge from Rad6 simultaneously (Fig. 3*E* and the purple line compared to the magenta and blue lines in Fig. 3*F*). Together, these results showed that Rtf1 promotes H2Bub, probably in part via accelerating ubiquitin discharge from Rad6.

The data showing that both Cdc73 (Fig. 2 *D* and *E*) and Rtf1 (Fig. 3 *E* and *F*) appear to stimulate ubiquitin discharge from Rad6 indicate that Cdc73 and Rtf1 might accelerate ubiquitin discharge from Rad6 simultaneously. To this end, we used an E2 discharge assay. Our results clearly showed that the rate of ubiquitin discharge from Rad6 after the addition of both the Cdc73 Ras-like domain and Rtf1, as indicated by Cdc73$^{(155-393)}$/Rtf1, was increased compared to that after the addition of either the Ras-like domain [Cdc73$^{(155-393)}$] or Rtf1 [Cdc73$^{(155-211)}$/Rtf1] (Fig. 3*G* and the purple line compared to the green or magenta line in Fig. 3*H*). Importantly, we found that the rate of ubiquitin discharge from Rad6 was further increased after the addition of Bre1 into the Ras-like domain and Rtf1, as indicated by Cdc73$^{(155-393)}$/Rtf1+Bre1 (Fig. 3*G* and the cyan line compared to purple line in Fig. 3*H*), indicating that Cdc73, Rtf1, and Bre1 accelerate ubiquitin discharge from Rad6 simultaneously. To further evaluate the important role of Cdc73 or Rtf1 in accelerating ubiquitin discharge from Rad6 in the context of holo-PAF1C, we prepared wild-type holo-PAF1C, PAF1C$_{\Delta\text{HMD}}$ (Rtf1 lacking the HMD), PAF1C$_{\Delta\text{Ras-like}}$ (Cdc73 lacking the Ras-like domain), and PAF1C$_{\Delta\text{HMD/Ras-like}}$ (Rtf1 lacking the HMD and Cdc73 lacking the Ras-like domain) (*SI Appendix*, Fig. S8*B*, lanes 1 through 4, respectively) and tested the ability of these complexes to accelerate ubiquitin discharge from Rad6. The results showed that the discharge efficiency was decreased after deletion of either the HMD (PAF1C$_{\Delta\text{HMD}}$) or Ras-like domain (PAF1C$_{\Delta\text{Ras-like}}$) (*SI Appendix*, Fig. S8*C* and the blue or magenta line compared to the purple line in *SI Appendix*, Fig. S8*D*) and that deletion of both the HMD and Ras-like domain (PAF1C$_{\Delta\text{HMD/Ras-like}}$) almost abolished the ability of PAF1C to

BIOCHEMISTRY

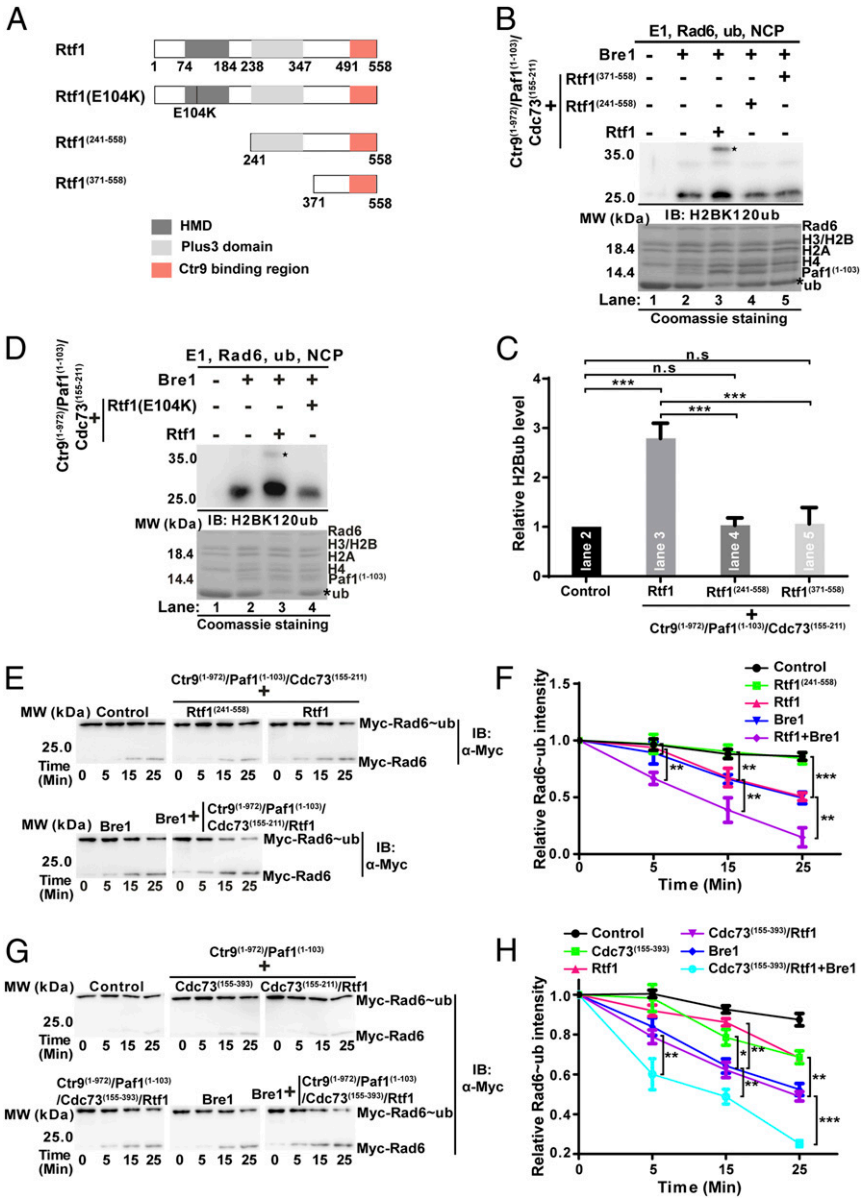

Fig. 3. Rtf1 HMD accelerates ubiquitin discharge from Rad6. (*A*) A schematic diagram of the full-length Rtf1 and two fragments of the mutant Rtf1(E104K). The HMD (gray), Plus-3 domain (light gray), and Ctr9-binding region (salmon) are shown in Rtf1. (*B* and *C*) Rtf1 HMD stimulates H2Bub, and (*D*) the binding of Rtf1 to Rad6 is important for stimulating H2Bub by Rtf1. An in vitro NCP ubiquitination assay was performed by adding various purified complexes, as indicated (*B* and *D*). The reactants were incubated for 90 min at 30 °C and analyzed by SDS-PAGE. The top half of the gel was immunoblotted with anti-H2B-K120ub antibody to specifically detect H2B-K120ub, and the bottom half of the gel was stained with Coomassie blue to confirm equal input of the NCPs. The bands representing ubiquitin and diubiquitinated H2B are marked with an asterisk and a star, respectively, in *B* and *D*. (*C*) Quantification of the in vitro NCP ubiquitination assay results in *B*. The intensity of the H2Bub band was quantified using ImageJ software. A control (lane 2 in *B*) was used for normalization. (*E* and *F*) Rtf1 HMD accelerates ubiquitin discharge from Rad6. (*E*) Representative immunoblot analysis of a single-turnover ubiquitin discharge experiment in which precharged Myc-Rad6~ub was incubated without or with Bre1 and/or various purified complexes as indicated at a final concentration of 3 μM. Aliquots were collected after 0, 5, 15, and 25 min of denaturation. The samples were separated by nonreducing SDS-PAGE followed by anti-Myc immunoblotting. (*G* and *H*) Cdc73, Rtf1, and Bre1 simultaneously accelerate ubiquitin discharge from Rad6. (*G*) Representative immunoblot from a single-turnover ubiquitin discharge experiment in which precharged Myc-Rad6~ub was incubated without or with Bre1 (3 μM) and/or various purified complexes (1 μM) as indicated. Aliquots were collected after 0, 5, 15, and 25 min of denaturation. The samples were separated by nonreducing SDS-PAGE followed by anti-Myc immunoblotting. (*F* and *H*) Quantification of the turnover experiments in *E* and *G*, respectively. The intensity of the Myc-Rad6~ub band was quantified using ImageJ software, and the intensity at time 0 was used for normalization. Error bars indicate the mean and SD (mean ± SD) ($n = 3$ of *C*, *E*, and *G*, separate experiments). n.s, not significant, $^{*}P < 0.05$, $^{**}P < 0.01$, $^{***}P < 0.001$.

accelerate ubiquitin discharge from Rad6 (*SI Appendix*, Fig. S8*C* and the green line compared to the purple and black lines in *SI Appendix*, Fig. S8*D*). Collectively, these results clearly indicated that Cdc73 and Rtf1 simultaneously accelerate ubiquitin discharge from Rad6 in the context of holo-PAF1C.

The Paf1/Leo1 Heterodimer Promotes H2Bub by Recognizing the Histone H3 Tail. In vitro H2Bub analysis showed that the level of H2Bub was higher with the addition of PAF1C$_{\Delta Rtf1}$ than with the addition of Ctr9$^{(1-972)}$/Paf1$^{(1-103)}$/Cdc73 (Fig. 1*F*, lane 4 compared to lane 6, and Fig. 1*G*), which, together with the fact that

the only difference between these two complexes is that the former includes the Paf1/Leo1 heterodimer, suggested that the Paf1/Leo1 heterodimer may be involved in PAF1C-induced stimulation of Rad6/Bre1-mediated H2Bub. Accordingly, several truncated Paf1 and Leo1 constructs were incorporated into $PAF1C_{\Delta Rtf1}$ complexes (Fig. 4 *A* and *B*). As anticipated, the level of H2Bub was higher with the addition of $PAF1C_{\Delta Rtf1}$ (containing the Ras-like domain of Cdc73) than with the addition of $Ctr9^{(1-972)}$/$Cdc73^{(1-211)}$/Paf1/Leo1 (without the Ras-like domain of Cdc73 and Rtf1 HMD) (Fig. 4*C*, lane 3 compared to lane 4, and Fig. 4*D*). Interestingly, the level of H2Bub after the addition of $Ctr9^{(1-972)}$/$Cdc73^{(1-211)}$/Paf1/Leo1 was higher than that after the addition of the control (without the PAF1C) (Fig. 4*C*, lane 4 compared to lane 2, and Fig. 4*D*). Notably, the level of H2Bub was decreased when the carboxyl-terminal region of Paf1 and the N-terminal and carboxyl-terminal regions of Leo1 were truncated separately or simultaneously (Fig. 4*C*, lanes 5 through 7 compared to lane 2, and Fig. 4*D*). Together, these results indicated that the carboxyl-terminal region of Paf1 and the N-terminal and carboxyl-terminal regions of Leo1 are important for the PAF1C-induced stimulation of H2Bub. This observation, together with the finding from a prior study showing that the Paf1/Leo1 heterodimer is necessary for the binding of PAF1C to a histone octamer or nucleosomes by the specific recognition of histone H3 (49), indicated that PAF1C-stimulated H2Bub might occur through PAF1C serving as a scaffold hub for Rad6/Bre1 and nucleosomal substrates. To test this hypothesis, the N-terminal 28 aa of histone H3 were fused to the N terminus of GST [$H3^{(1-28)}$-GST]. As anticipated, GST pull-down analysis showed that $PAF1C_{\Delta Rtf1}$ (containing the intact Paf1/Leo1 heterodimer), but not the Paf1 subcomplexes in which the N-terminal and carboxyl-terminal region were removed from Leo1 alone or together with Paf1 in which the carboxyl-terminal region was removed, specifically bound the H3 tail (Fig. 4*E*, lane 2 compared to lanes 4 and 5). The Paf1 subcomplex containing Paf1 in which the carboxyl-terminal region had been removed alone can bind the H3 tail (lane 3 in Fig. 4*E*). It is unclear that this subcomplex lost its ability to stimulate H2Bub in vitro (Fig. 4*C*, lane 5 compared to lane 3, and Fig. 4*D*).

Next, we tested the role of H3 binding of the Paf1/Leo1 heterodimer in promoting H2Bub in vivo. We found that the level of H2Bub is decreased in yeast lacking either PAF1 gene (*paf1Δ*), LEO1 gene (*leo1Δ*), or both PAF1 gene and LEO1 gene (*paf1Δleo1Δ*) (Fig. 4*F*, lanes 2, 7, or 5, respectively, compared to lane 1, and Fig. 4*G*) and that the expression of either wild-type Paf1 (*Paf1-WT*) in the *paf1Δ* yeast strain or wild-type Leo1 (*Leo1-WT*) in the *leo1Δ* yeast strain fully restored the levels of H2Bub (Fig. 4*F*, lane 3 or 8 compared to lane 1, respectively, and Fig. 4*G*). Notably, the expression of the mutant Leo1 (*Leo1ΔN,C*), which is incapable of binding to H3 tail (lane 4 in Fig. 4*E*) in the *leo1Δ* yeast strain could not fully restore the level of H2Bub (Fig. 4*F*, lane 9 compared to lane 8, and Fig. 4*G*). Additionally, the expression of the mutant Paf1 (*Paf1ΔC*), which is capable of binding to H3 tail (lane 3 in Fig. 4*E*) in the *paf1Δ* yeast strain largely restored H2Bub (Fig. 4*F*, lane 4 compared to lane 3, and Fig. 4*G*), whereas the expression of the mutant Paf1ΔC in the *paf1Δleo1Δ* yeast strain, in which PAF1C is incapable of binding to H3 tail (lane 5 in Fig. 4*E*), only slightly restored the level of H2Bub (Fig. 4*F*, lane 6 compared to lane 1, and Fig. 4*G*). Collectively, these results clearly demonstrated that the binding of the Paf1/Leo1 heterodimer to nucleosomal substrates might play an important role in maintaining the normal level of H2Bub in vivo.

Discussion

Our biochemical data revealed that the extreme carboxyl terminus of Rtf1 [$Rtf1^{(491-558)}$] stably binds the middle region of Ctr9 [$Ctr9^{(313-477)}$] (*SI Appendix*, Fig. S3 *B–E*). Consistent with our finding, a prior cross-linking assay showed that the carboxyl terminus of human Rtf1 interacts with TPR-5, -6, -7, and -11 of Ctr9 (45), indicating that the interaction between Rtf1 and Ctr9 is extensively conserved from yeast to humans.

Importantly, the results from an established, transcription-free, minimal in vitro ubiquitination system clearly demonstrated the following: 1) the binding of Ctr9 to the eight extreme carboxyl-terminal residues of the acidic tail of Rad6 is required for PAF1C-induced stimulation of H2Bub (Fig. 1 and *SI Appendix*, Fig. S6); 2) through a function, the Ras-like domain of Cdc73 directly binds Rad6 and has the potential to accelerate ubiquitin discharge from Rad6 (Figs. 2 and 5*A* and *SI Appendix*, Fig. S7*B*); 3) Rtf1 HMD might accelerate ubiquitin discharge from Rad6 alone or in cooperation with Cdc73, depending on its interaction with Rad6 (Figs. 3 and 5*B*); and 4) specific recognition of the histone H3 tail of the nucleosomal substrates by the Paf1/Leo1 heterodimer is important for PAF1C-stimulated Rad6/Bre1-mediated H2Bub (Figs. 4 and 5*C*). Collectively, these results, as well as the observation showing that the Ctr9/Paf1 heterodimer is required for PAF1C assembly (refs. 46 and 49) and those of prior studies indicating a role for PAF1C-mediated transcriptional regulation (refs. 31, 41, and 56), led to the establishment of a model for the assembly of yeast PAF1C and PAF1C-induced stimulation of Rad6/Bre1-mediated H2Bub in the context of the Pol II transcription complex (Fig. 5*D*).

Our work revealed that PAF1C makes multivalent interactions with Rad6, which are essential for accelerating ubiquitin discharge from Rad6 and stimulating H2Bub in vitro and in vivo. More importantly, the Cdc73 Ras-like domain and the Rtf1 HMD appear to have the potential to stimulate discharge of ubiquitin from Rad6, which might be further enhanced in the presence of Bre1. It seems to indicate that PAF1C and Bre1 may interact with Rad6 simultaneously (*SI Appendix*, Fig. S5 *F* and *G*) and form a functional complex (Figs. 1–4). However, the detailed mechanisms for Cdc73 and Rtf1 binding Rad6 are limited, and future studies are necessary to be explored.

Prior studies showed that either human or yeast PAF1C failed to stimulate H2Bub in reconstituted ubiquitination systems containing nucleosomes purified from HeLa cells (33, 41). We clearly demonstrated that yeast PAF1C promotes Rad6/Bre1-mediated H2Bub through an established in vitro ubiquitination assay (Fig. 1*B*); the ability to make these observations presumably relates to our use of recombinant substrate nucleosomes devoid of preexisting marks. The ability of the human Cdc73 Ras-like domain to promote H2Bub (*SI Appendix*, Fig. S7*B*), together with the observations suggesting that the level of H2Bub is decreased in the context of the ubiquitination system containing either mutant Rtf1 (E104K) [abolishing the H2Bub in yeast (31)] (Fig. 3*D*) or $Rad6^{(1-164)}$ (inability to bind to Ctr9) (*SI Appendix*, Fig. S6 *A–C*), supported the supposition that PAF1C has functional significance in promoting Rad6/Bre1-mediated H2Bub.

In summary, intact PAF1C is required to efficiently stimulate Rad6/Bre1-mediated H2Bub, which is consistent with the observation that expressing Rtf1 only partially restores normal H2Bub levels in the context of the absence of all other PAF1C subunits (31). Future studies are necessary to further evaluate this model in vivo and in other species and to assess the structures involved in Pol II transcription–coupled H2Bub in different combinations (e.g., PAF1C with Rad6~ub and/or Bre1 or with nucleosomes) or in different states. Moreover, it will be interesting to determine whether PAF1C is involved and plays a similar role in ubiquitination that is not mediated through Rad6/Bre1.

Materials and Methods

Protein Expression and Purification. All DNA fragments of proteins involved in this study were from the *S. cerevisiae* genome and were amplified by PCR. To coexpress a fragment of yeast Ctr9 [residues 1 through 972, $Ctr9^{(1-972)}$], yeast Paf1 [residues 1 through 103, $Paf1^{(1-103)}$], yeast Cdc73 [residues 155 through 211, $Cdc73^{(155-211)}$], $Ctr9^{(1-972)}$, and $Paf1^{(1-103)}$ were inserted sequentially into

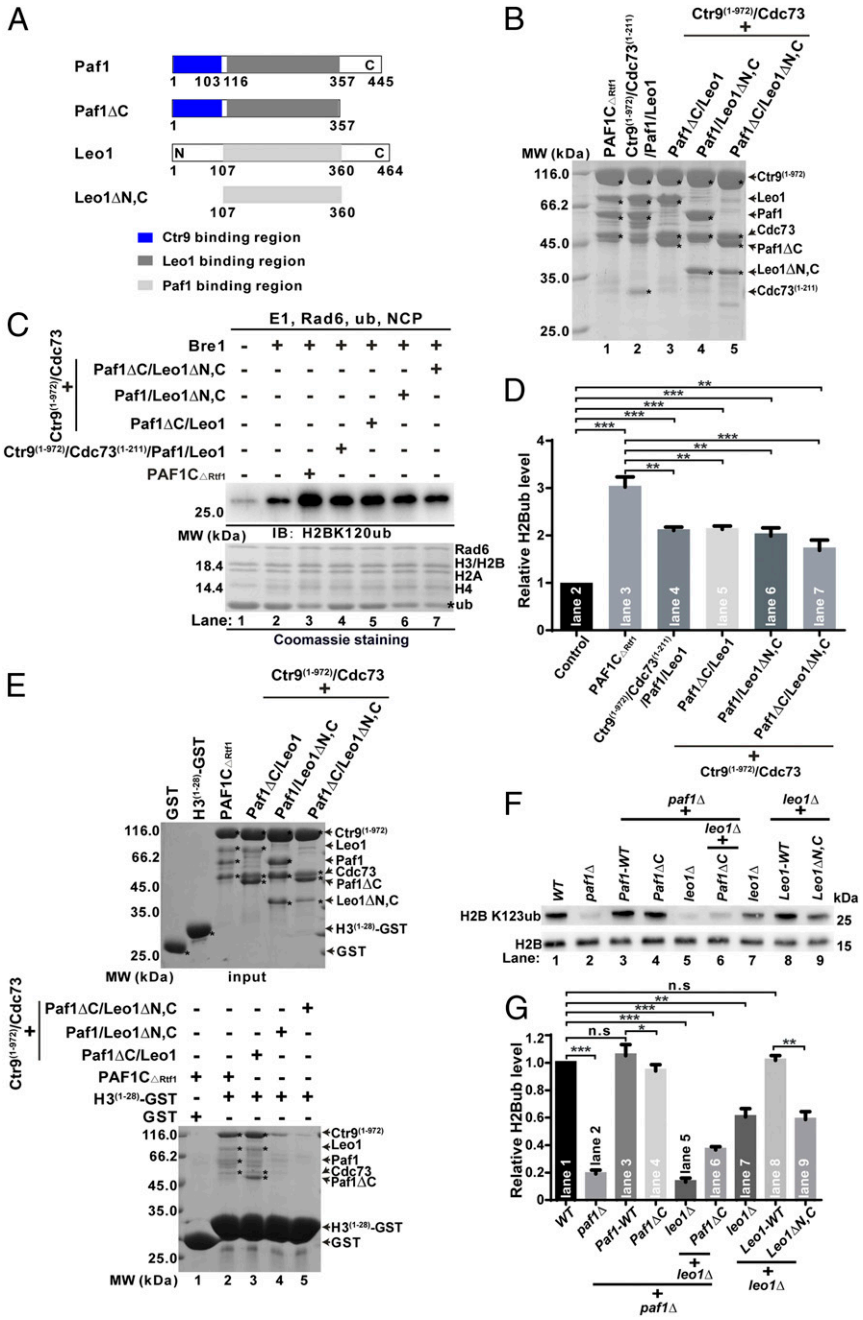

Fig. 4. The Paf1/Leo1 heterodimer stimulates H2Bub by recognizing the histone H3 tail of nucleosomal substrates. (*A*) A schematic representation of various fragments of the subunits Paf1 and Leo1 that were coexpressed with Ctr9$^{(1-972)}$/Cdc73 [or Cdc73$^{(1-211)}$] is shown. The Ctr9-binding region (blue) and Leo1-binding region (gray) in Paf1 are shown. The Paf1-binding region (light gray) in Leo1 is shown. (*B*) SDS-PAGE analysis of purified PAF1C$_{\Delta Rtf1}$ and various Paf1 subcomplexes as indicated. (*C* and *D*) The Paf1/Leo1 heterodimer stimulates H2Bub. (*C*) An in vitro NCP ubiquitination assay was performed by adding the indicated complexes (lanes 3 through 7 in *C*). The reactants were incubated for 90 min at 30 °C and analyzed by SDS-PAGE. The top half of the gel was immunoblotted with anti-H2B-K120ub antibody to specifically detect H2B-K120ub, and the bottom half of the gel was stained with Coomassie blue to confirm equal input of the NCPs. The ubiquitin band is marked with an asterisk. (*D*) Quantification of the in vitro NCP ubiquitination assay results in *C*. The intensity of the H2Bub band was quantified using ImageJ software. A control (lane 2 in *C*) was used for normalization. Error bars indicate the mean and SD (mean ± SD) ($n = 3$, separate experiments). (*E*) GST pull-down assays of purified complexes with histone H3 tails. H3$^{(1-28)}$-GST fusion proteins were incubated with various Paf1 complexes, as indicated in the right panel, for 1 h at 4 °C. The prepared samples were separated by SDS-PAGE and stained with Coomassie blue. Input of the purified Paf1 subcomplexes is shown in the top panel. (*F*) The human anti-H2B-K120ub antibody can also specifically detect the H2B-K123ub in yeast (*Top*) or with anti-H2B antibody to confirm equal loading (*Bottom*). (*G*) Quantification of the intensity of H2Bub bands shown in *F*. Three independent experiments were performed for *F* and used for quantification. The error bars indicate the mean and SD (mean ± SD) ($n = 3$, separate experiments). n.s, not significant, $*P < 0.05$, $**P < 0.01$, $***P < 0.001$.

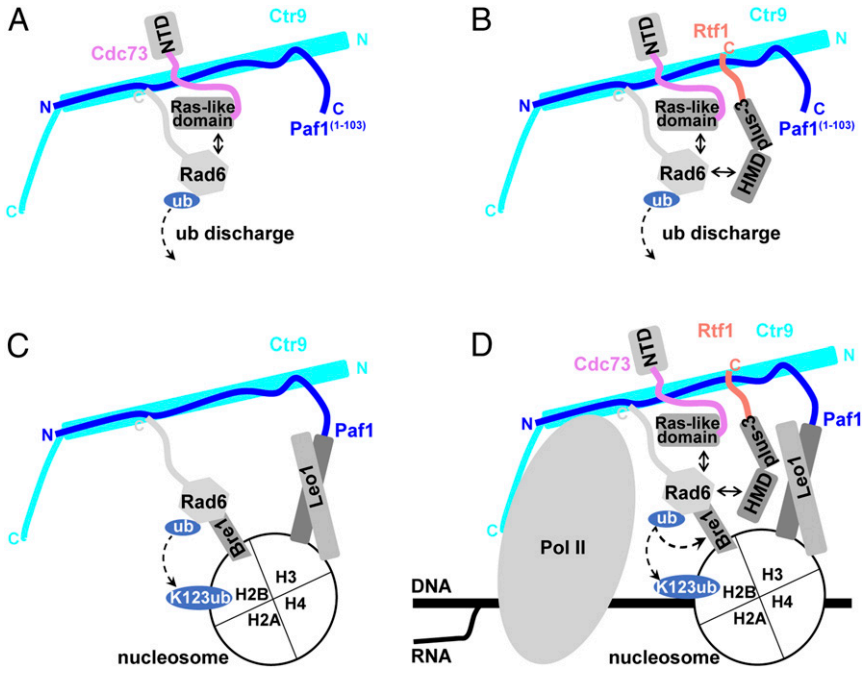

Fig. 5. Schematic model of yeast PAF1C-induced stimulation of Rad6/Bre1-mediated H2Bub in the context of transcription. (*A* and *B*) The reaction schemes showing Cdc73 (*A*) and Rtf1 (*B*) accelerating ubiquitin discharge from Rad6. NTD, N-terminal domain of Cdc73. (*C*) The reaction scheme of the Paf1/Leo1 heterodimer (46) stimulating H2Bub by specifically recognizing the H3 tail of the nucleosomal substrates. (*D*) Ctr9 acts as a hub in PAF1C-induced stimulation of Rad6/Bre1-mediated H2Bub by simultaneous Rtf1, Cdc73, and Bre1 acceleration of ubiquitin discharge from Rad6 and by Paf1/Leo1 heterodimer recognizing nucleosomal substrates and in binding the Pol II transcriptional complex (only Pol II is shown for clarity, and ref. 56). The two-way arrow represents the interaction between Rad6 and Cdc73 or between Rad6 and Rtf1 HMD (31). The dashed arrow indicates the ubiquitin discharge from Rad6 to Bre1 and K123 of H2B.

two multiple cloning sites of an in-house-modified version of the pETDuet-1 vector (Novagen). $Cdc73^{(155-211)}$ was cloned into an in-house modified version of the pET-32a vector (Novagen). Ribosome binding sequence (RBS)-$Cdc73^{(155-211)}$, which contains an RBS on the N terminus of $Cdc73^{(155-211)}$, was inserted sequentially behind $Paf1^{(1-103)}$. For coexpression of the quaternary complex of $Ctr9^{(1-972)}$/$Paf1^{(1-103)}$/$Cdc73^{(155-211)}$/$Rtf1^{(491-558)}$, yeast Rtf1 [residues 491 through 558, $Rtf1^{(491-558)}$] was inserted behind $Ctr9^{(1-972)}$ by the same strategy used to insert $Cdc73^{(155-211)}$. For coexpression of the quaternary complex of $Ctr9^{(1-972)}$/Paf1/Cdc73/Leo1, full-length yeast Leo1 was inserted behind $Ctr9^{(1-972)}$ by the same strategy used to insert $Cdc73^{(155-211)}$ and $Rtf1^{(491-558)}$. All of the resulting proteins contained a thioredoxin (Trx)-his6 tag on the N terminus.

BL21(DE3)-pUBS520 *Escherichia coli* (*E. coli*) cells containing the expression plasmids were grown in lysogeny broth (LB) medium at 37 °C until the optical density at the 600 nm (OD600) absorbance value reached 1.0, and then these cells were induced with 0.3 mM isopropyl-β-D-thiogalactoside at 16 °C for 16 to 18 h. The cells were harvested by centrifugation at 4,000 rpm for 20 min. The cells were washed and resuspended in buffer containing 50 mM Tris-HCl, pH 8.0; 400 mM NaCl; and 10 mM imidazole and then lysed by an AH-1500 high-pressure cell homogenizer (ATS Engineering Limited). The Trx-his6-tagged protein complex was purified on a HisTrap HP 5-mL column (GE Healthcare) followed by size-exclusion chromatography on a HiLoad 26/60 Superdex200 (GE Healthcare) with 50 mM Tris-HCl, pH8.0; 100 mM NaCl; 1 mM ethylenediaminetetraacetic acid (EDTA); and 1 mM dithiothreitol (DTT). After digestion with PreScission protease to cleave the N-terminal Trx-his6 tag, the target protein was further purified on a HiTrap Q HP 16/10 anion-exchange column. The final purification step was size-exclusion chromatography on a Superdex 200 10/300 increase column (GE Healthcare) in 50 mM Tris-HCl, pH 8.0; 100 mM NaCl; and 1 mM DTT.

Various other Paf1 subcomplexes reported in this manuscript were prepared with similar coexpression and purification strategies, except PAF1C and three mutant PAF1Cs ($PAF1C_{\Delta HMD}$, $PAF1C_{\Delta Ras\text{-}like}$, and $PAF1C_{\Delta HMD/Ras\text{-}like}$). The PAF1C and mutant PAF1C recombinant proteins were prepared by colysing *E. coli* cells expressing $Ctr9^{(1-972)}$/Leo1/Paf1/Cdc73 with those expressing Rtf1.

The Uba1 (E1) DNA fragment was inserted into an in-house-modified version of the pET-32a vector, and the expressed Uba1 has a Trx-his6-tag on its N terminus and a his6-tag on its carboxyl terminus (Trx-His-Uba1-his6). Uba1 was purified on a HisTrap HP 5-mL column followed by size-exclusion chromatography on a HiLoad 26/60 Superdex200 in 50 mM Tris-HCl, pH 8.0; 50 mM NaCl; 50 mM KCl; 10 mM $MgCl_2$; and 1 mM DTT. After digestion with PreScission protease to cleave the N-terminal Trx-his6 tag, Uba1 was further purified on a HisTrap HP 5-mL column by using an imidazole gradient (0.01 to 0.25 M). The final purification step was size-exclusion chromatography on a Superdex 200 10/300 increase column in 50 mM Tris-HCl, pH 8.0; 50 mM NaCl; 50 mM KCl; and 10 mM $MgCl_2$. Bre1 (E3) was prepared with similar expression and purification strategies.

Recombinant Rad6 (E2) or Myc-Rad6 and ubiquitin or Myc-ubiquitin were expressed and purified as previously described (57).

Histone Octamer Purification and Nucleosome Core Particle Reconstitution. Human nucleosome core particles (NCPs) were reconstituted from human histone octamers and 147-bp DNA containing the "WIDOM 601" positioning sequence (5′- ATCAATATCCACCTGCAGATACTACCAAAAGTGTATTTGGAAACTGCTCCATCAAAAGGCATGTTCAGCTGGAATCCAGCTGAACATGCCTTTTGATGGAGCAGTTTCCAAATACACTTTTGGTAGTATCTGCAGGTGGATATTGAT-3′) according to a modified method (58). The respective histones were expressed in *E. coli* BL21 (DE3) and isolated as inclusion bodies. The inclusion bodies were solubilized in buffer (50 mM Tris-HCl, pH 7.5; 6 M guanidine hydrochloride; and 500 mM NaCl) overnight and further purified on a HisTrap HP 5-mL column by using an imidazole gradient (0.01 to 0.4 M). Equimolar amounts of individual purified histones were dialyzed into denature buffer (20 mM Tris-HCl, pH 7.5; 7 M guanidine hydrochloride; and 10 mM DTT) overnight and further dialyzed into refolding buffer (10 mM Tris-HCl, pH 7.5; 2 M NaCl; 2 mM EDTA; and 5 mM DTT). After digestion with PreScission protease to cleave the N-terminal his6 tag, the refolded histone octamers were finally purified on a Superdex 200 10/300 increase column in refolding buffer. The NCP reconstitution reaction mixture containing octamers and 147-bp DNA were dialyzed over 16 h at 4 °C in buffer (10 mM Tris-HCl, pH 8.0; 1 mM EDTA; and 2 M KCl), which was continuously diluted by slowly adding TE (Tris-EDTA) buffer (10 mM Tris-HCl, pH 8.0; and 1 mM EDTA) to lower the concentration of KCl from 2 M to 0.25 M. After the gradient dilution has finished, NCPs were dialyzed for at least 3 h in buffer (10 mM Tris-HCl, pH 7.5; 0.25 M KCl; 1 mM EDTA; and 1 mM DTT). The reconstituted NCPs were further purified on a Superdex 200 10/300

increase column in buffer (10 mM Tris-HCl, pH 7.5; 50 mM KCl; 1 mM EDTA; and 1 mM DTT) and then stored in small aliquots at −80 °C.

Protein Interaction Assays. For GST pull-down assays, GST-Rad6, GST-Rad6$^{(1-149)}$, GST-Bre1^{RBD}, and H3$^{(1-28)}$-GST fusion proteins were expressed in *E. coli* BL21(DE3) Codon Plus cells and purified using a glutathione-Sepharose 4B column (GE Healthcare) and a HiLoad 26/60 Superdex 200 column with 50 mM Tris-HCl, pH 8.0; 100 mM NaCl; and 1 mM DTT. The mixture of purified GST fusion proteins and indicated proteins were incubated with glutathione-Sepharose 4B beads in buffer (50 mM Tris-HCl, pH 8.0; 100 mM NaCl; 5% glycerol; and 0.5% Triton X-100) at 4 °C for 1 h. The beads were collected by centrifugation and washed three times with the same buffer. For size-exclusion chromatography analysis, purified Paf1 subcomplexes were mixed with Rad6, Rad6$^{(1-149)}$, or Rad6$^{(1-164)}$ in buffer composed of 50 mM Tris-HCl, pH 8.0; 100 mM NaCl; and 1 mM DTT at 4 °C. Complexes were separated by an analytical size-exclusion column pre-equilibrated in buffer (50 mM Tris-HCl, pH 8.0; 100 or 200 mM NaCl; and 1 mM DTT). The prepared samples from the GST pull-down assays or size-exclusion chromatography analysis were separated by SDS-PAGE, and the gels were stained with Coomassie blue.

In Vitro NCP Ubiquitination Assay. For NCP ubiquitination reactions, 100 nM E1 (Uba1), 2 μM Rad6, 36 μM ubiquitin, 10 μM Bre1, 3 μM PAF1C or other indicated subcomplexes, 3 mM ATP (adenosine triphosphate), and 0.1 mM DTT were mixed in a total volume of 20 μL in buffer (50 mM Tris-HCl, pH 8.0; 50 mM NaCl; 50 mM KCl; and 10 mM $MgCl_2$) and incubated for 90 min at 30 °C (39). The reactions were stopped by adding 5× Laemmli sample buffer. To test the signals of H2B-K120ub, 10 μL of each sample was loaded and analyzed by SDS-PAGE followed by Western blotting with anti-H2B-K120ub antibody. To measure the ubiquitin signals, 2 μL of each sample was loaded for SDS-PAGE and assessed by Western blotting with an anti-Myc antibody.

Cross-Linking Assay. For the cross-linking assay, purified Rad6 was mixed with Cdc73$^{(1-211)}$ or Cdc73$^{(155-393)}$ by a molar ratio of 1:1 in buffer (25 mM Hepes, pH 7.5; 100 mM NaCl; and 1 mM DTT) at a final concentration of 5 μM. Samples were incubated at 4 °C, and aliquots were collected 1 min after supplementing with 0.1% (vol/vol) glutaraldehyde and denatured by adding 5× Laemmli sample buffer. Rad6, Cdc73$^{(1-211)}$, or Cdc73$^{(155-393)}$, as negative control, respectively, was cross-linked under the same conditions. All samples were loaded and analyzed by SDS-PAGE.

E2 Discharge Assay. We performed an E2 (Rad6) discharge assay according to a protocol published by Alwin Köhler (39). Precharging of Rad6 was performed with 250 nM E1 (Uba1), 45 μM ubiquitin, 2 μM Myc-Rad6 (the Myc-tag was used to measure the Rad6 band intensity after Western blotting), 0.2 mM DTT, and 3 mM ATP in buffer (50 mM Tris-HCl, pH 8.0; 50 mM NaCl; 50 mM KCl; and 10 mM $MgCl_2$) for 90 min at 30 °C. Precharging reactions were quenched by adding EDTA, pH 8.0, at a final concentration of 50 mM and placing the mixture on ice for 5 min. Various Paf1 subcomplexes and/or Bre1 were added to the precharging Rad6 mixture (Myc-Rad6∼ub) at a final concentration of 3 μM or 1 μM, as indicated in the figure legends, for a final reaction volume of 50 μL. Samples were incubated at 30 °C, and aliquots were collected after 0, 5, 15, and 25 min and denatured by adding 5× nonreducing Laemmli sample buffer. Then, 10 μL samples were loaded and analyzed by nonreducing SDS-PAGE followed by Western blotting. Quantification of the Myc-Rad6∼ub band intensity was performed with ImageJ software. Specifically, if the bands were normalized, the rectangular or oval selection option was used; if they were not normalized, the freehand option was used.

Western Blotting. All samples were separated by SDS-PAGE and transferred to polyvinylidene difluoride (PVDF) membranes (Millipore). The membranes were subsequently blocked overnight with 10% nonfat milk in TBST (Tris-buffered saline with 0.1% Tween 20, 50 mM Tris-HCl, pH 7.5; 150 mM NaCl; and 0.1% Tween 20) at 4 °C. The PVDF membranes were immunoblotted with anti-Myc antibody (Sigma, M4439; 1:5,000 dilution), anti-H2B antibody (Abcam, ab188271; 1:5,000 dilution), anti-H3 antibody (Abcam, ab1791; 1:5,000 dilution) or anti-H2B-K120ub antibody (Cell Signaling No. 5546; 1:1,000 dilution) at 4 °C for 1 h, probed with horseradish peroxidase–conjugated secondary antibodies at a dilution of 1:5,000 (Santa Cruz, sc-2004 and sc-2005) and developed with a chemiluminescent substrate (Millipore). Protein bands were visualized on the Tanon-5200 Chemiluminescent Imaging System (Tanon Science and Technology). All experiments were repeated at least three times.

Yeast Culture and Growth Conditions. Yeast cells were grown in rich YPD (yeast extract peptone dextrose medium, 1% yeast extract, 2% peptone, and 2% glucose) or synthetic minimal medium (0.67% yeast nitrogen base, 2% glucose, and amino acids as needed) at 30 or 37 °C. In some experiments, cells were also cultured in the presence of 0.5 M NaCl or 100 mM HU.

H2B K123ub In Vivo. The *S. cerevisiae* strains used in this study are summarized in *SI Appendix*, Table S1. Yeast cells were grown in YPD medium to stable log phase (OD600 ∼ 0.6 to 1.0) at 30 °C. Then, an equivalent number of OD units was harvested for each strain and washed in TE buffer (10 mM Tris-HCl, pH 8.0, and 1 mM EDTA) once. The pellets were resuspended in 100 μL SUTEB buffer (1% SDS; 8 M Urea; 10 mM Tris-HCl, pH 8.0; 10 mM EDTA; and 0.01% bromophenol blue) and boiled for 5 min. Yeast cells were lysed by glass beads beating for 30 min, and the extracts were centrifuged for clarifying. Samples were loaded on SDS-PAGE gels, followed by immunoblotting with anti-H2B antibody (Abcam, ab188271; 1:5,000 dilution) and anti-H2B-K120ub antibody (Cell Signaling No. 5546; 1:1,000 dilution).

Data Availability. All data are included in this manuscript and/or *SI Appendix*.

ACKNOWLEDGMENTS. This work was supported by National Natural Science Foundation of China Grant Nos. 31870750 to H.Z. and 31670758 to J.L.; by Natural Science Foundation of Tianjin Grant No. 20JCYBJC01320 to J.L.; and by Fundamental Research Funds for the Central Universities, Nankai University Grant No. 030/63211052 to J.L.

1. S. B. Van Oss, C. E. Cucinotta, K. M. Arndt, Emerging insights into the roles of the Paf1 complex in gene regulation. *Trends Biochem. Sci.* **42**, 788–798 (2017).
2. B. Zhu *et al.*, The human PAF complex coordinates transcription with events downstream of RNA synthesis. *Genes Dev.* **19**, 1668–1673 (2005).
3. H. Gaillard *et al.*, Genome-wide analysis of factors affecting transcription elongation and DNA repair: A new role for PAF and Ccr4-not in transcription-coupled repair. *PLoS Genet.* **5**, e1000364 (2009).
4. P. Herr *et al.*, A genome-wide IR-induced RAD51 foci RNAi screen identifies CDC73 involved in chromatin remodeling for DNA repair. *Cell Discov.* **1**, 15034 (2015).
5. I. Kikuchi *et al.*, Dephosphorylated parafibromin is a transcriptional coactivator of the Wnt/Hedgehog/Notch pathways. *Nat. Commun.* **7**, 12887 (2016).
6. H. Fischl, F. S. Howe, A. Furger, J. Mellor, Paf1 has distinct roles in transcription elongation and differential transcript fate. *Mol. Cell* **65**, 685–698.e8 (2017).
7. C. Koch, P. Wollmann, M. Dahl, F. Lottspeich, A role for Ctr9p and Paf1p in the regulation G1 cyclin expression in yeast. *Nucleic Acids Res.* **27**, 2126–2134 (1999).
8. L. Ding *et al.*, A genome-scale RNAi screen for Oct4 modulators defines a role of the Paf1 complex for embryonic stem cell identity. *Cell Stem Cell* **4**, 403–415 (2009).
9. L. Zheng *et al.*, The Paf1 complex transcriptionally regulates the mitochondrial-anchored protein Atg32 leading to activation of mitophagy. *Autophagy* **16**, 1366–1379 (2020).
10. A. G. Muntean *et al.*, The PAF complex synergizes with MLL fusion proteins at HOX loci to promote leukemogenesis. *Cancer Cell* **17**, 609–621 (2010).
11. K. Hetzner, M. P. Garcia-Cuellar, C. Büttner, R. K. Slany, The interaction of ENL with PAF1 mitigates polycomb silencing and facilitates murine leukemogenesis. *Blood* **131**, 662–673 (2018).
12. R. K. Nimmakayala *et al.*, Cigarette smoke induces stem cell features of pancreatic cancer cells via PAF1. *Gastroenterology* **155**, 892–908.e6 (2018).
13. S. Karmakar *et al.*, PD2/PAF1 at the crossroads of the cancer network. *Cancer Res.* **78**, 313–319 (2018).
14. H. H. Ng, S. Dole, K. Struhl, The Rtf1 component of the Paf1 transcriptional elongation complex is required for ubiquitination of histone H2B. *J. Biol. Chem.* **278**, 33625–33628 (2003).
15. N. J. Krogan *et al.*, The Paf1 complex is required for histone H3 methylation by COMPASS and Dot1p: Linking transcriptional elongation to histone methylation. *Mol. Cell* **11**, 721–729 (2003).
16. A. Wood, J. Schneider, J. Dover, M. Johnston, A. Shilatifard, The Paf1 complex is essential for histone monoubiquitination by the Rad6-Bre1 complex, which signals for histone methylation by COMPASS and Dot1p. *J. Biol. Chem.* **278**, 34739–34742 (2003).
17. H. H. Ng, F. Robert, R. A. Young, K. Struhl, Targeted recruitment of Set1 histone methylase by elongating Pol II provides a localized mark and memory of recent transcriptional activity. *Mol. Cell* **11**, 709–719 (2003).
18. Y. Chu, R. Simic, M. H. Warner, K. M. Arndt, G. Prelich, Regulation of histone modification and cryptic transcription by the Bur1 and Paf1 complexes. *EMBO J.* **26**, 4646–4656 (2007).
19. B. N. Tomson, C. P. Davis, M. H. Warner, K. M. Arndt, Identification of a role for histone H2B ubiquitylation in noncoding RNA 3′-end formation through mutational analysis of Rtf1 in *Saccharomyces cerevisiae*. *Genetics* **188**, 273–289 (2011).
20. L. Moyal *et al.*, Requirement of ATM-dependent monoubiquitylation of histone H2B for timely repair of DNA double-strand breaks. *Mol. Cell* **41**, 529–542 (2011).
21. L. Wu, L. Li, B. Zhou, Z. Qin, Y. Dou, H2B ubiquitylation promotes RNA Pol II processivity via PAF1 and pTEFb. *Mol. Cell* **54**, 920–931 (2014).

22. S. D. Briggs *et al*., Gene silencing: Trans-histone regulatory pathway in chromatin. *Nature* **418**, 498 (2002).
23. J. Dover *et al*., Methylation of histone H3 by COMPASS requires ubiquitination of histone H2B by Rad6. *J. Biol. Chem.* **277**, 28368–28371 (2002).
24. H. H. Ng, R. M. Xu, Y. Zhang, K. Struhl, Ubiquitination of histone H2B by Rad6 is required for efficient Dot1-mediated methylation of histone H3 lysine 79. *J. Biol. Chem.* **277**, 34655–34657 (2002).
25. Z. W. Sun, C. D. Allis, Ubiquitination of histone H2B regulates H3 methylation and gene silencing in yeast. *Nature* **418**, 104–108 (2002).
26. C. K. Govind *et al*., Phosphorylated Pol II CTD recruits multiple HDACs, including Rpd3C(S), for methylation-dependent deacetylation of ORF nucleosomes. *Mol. Cell* **39**, 234–246 (2010).
27. T. Kim, S. Buratowski, Dimethylation of H3K4 by Set1 recruits the Set3 histone deacetylase complex to 5′ transcribed regions. *Cell* **137**, 259–272 (2009).
28. D. G. Martin *et al*., The Yng1p plant homeodomain finger is a methyl-histone binding module that recognizes lysine 4-methylated histone H3. *Mol. Cell. Biol.* **26**, 7871–7879 (2006).
29. N. Minsky *et al*., Monoubiquitinated H2B is associated with the transcribed region of highly expressed genes in human cells. *Nat. Cell Biol.* **10**, 483–488 (2008).
30. V. M. Weake, J. L. Workman, Histone ubiquitination: Triggering gene activity. *Mol. Cell* **29**, 653–663 (2008).
31. S. B. Van Oss *et al*., The histone modification domain of Paf1 complex subunit Rtf1 directly stimulates H2B ubiquitylation through an interaction with Rad6. *Mol. Cell* **64**, 815–825 (2016).
32. G. Fuchs, D. Hollander, Y. Voichek, G. Ast, M. Oren, Cotranscriptional histone H2B monoubiquitylation is tightly coupled with RNA polymerase II elongation rate. *Genome Res.* **24**, 1572–1583 (2014).
33. J. Kim *et al*., RAD6-mediated transcription-coupled H2B ubiquitylation directly stimulates H3K4 methylation in human cells. *Cell* **137**, 459–471 (2009).
34. B. Fierz *et al*., Histone H2B ubiquitylation disrupts local and higher-order chromatin compaction. *Nat. Chem. Biol.* **7**, 113–119 (2011).
35. A. B. Fleming, C. F. Kao, C. Hillyer, M. Pikaart, M. A. Osley, H2B ubiquitylation plays a role in nucleosome dynamics during transcription elongation. *Mol. Cell* **31**, 57–66 (2008).
36. R. Pavri *et al*., Histone H2B monoubiquitination functions cooperatively with FACT to regulate elongation by RNA polymerase II. *Cell* **125**, 703–717 (2006).
37. A. Wood *et al*., Bre1, an E3 ubiquitin ligase required for recruitment and substrate selection of Rad6 at a promoter. *Mol. Cell* **11**, 267–274 (2003).
38. K. Robzyk, J. Recht, M. A. Osley, Rad6-dependent ubiquitination of histone H2B in yeast. *Science* **287**, 501–504 (2000).
39. E. Turco, L. D. Gallego, M. Schneider, A. Köhler, Monoubiquitination of histone H2B is intrinsic to the Bre1 RING domain-Rad6 interaction and augmented by a second Rad6-binding site on Bre1. *J. Biol. Chem.* **290**, 5298–5310 (2015).
40. L. D. Gallego *et al*., Structural mechanism for the recognition and ubiquitination of a single nucleosome residue by Rad6-Bre1. *Proc. Natl. Acad. Sci. U.S.A.* **113**, 10553–10558 (2016).
41. J. Kim, R. G. Roeder, Direct Bre1-Paf1 complex interactions and RING finger-independent Bre1-Rad6 interactions mediate histone H2B ubiquitylation in yeast. *J. Biol. Chem.* **284**, 20582–20592 (2009).
42. A. S. Piro, M. K. Mayekar, M. H. Warner, C. P. Davis, K. M. Arndt, Small region of Rtf1 protein can substitute for complete Paf1 complex in facilitating global histone H2B ubiquitylation in yeast. *Proc. Natl. Acad. Sci. U.S.A.* **109**, 10837–10842 (2012).
43. P. Deng *et al*., Transcriptional elongation factor Paf1 core complex adopts a spirally wrapped solenoidal topology. *Proc. Natl. Acad. Sci. U.S.A.* **115**, 9998–10003 (2018).
44. S. M. Vos *et al*., Structure of activated transcription complex Pol II-DSIF-PAF-SPT6. *Nature* **560**, 607–612 (2018).
45. S. M. Vos, L. Farnung, A. Linden, H. Urlaub, P. Cramer, Structure of complete Pol II-DSIF-PAF-SPT6 transcription complex reveals RTF1 allosteric activation. *Nat. Struct. Mol. Biol.* **27**, 668–677 (2020).
46. Y. Xie *et al*., Paf1 and Ctr9 subcomplex formation is essential for Paf1 complex assembly and functional regulation. *Nat. Commun.* **9**, 3795 (2018).
47. J. A. Jaehning, The Paf1 complex: Platform or player in RNA polymerase II transcription? *Biochim. Biophys. Acta* **1799**, 379–388 (2010).
48. B. N. Tomson, K. M. Arndt, The many roles of the conserved eukaryotic Paf1 complex in regulating transcription, histone modifications, and disease states. *Biochim. Biophys. Acta* **1829**, 116–126 (2013).
49. X. Chu *et al*., Structural insights into Paf1 complex assembly and histone binding. *Nucleic Acids Res.* **41**, 10619–10629 (2013).
50. M. H. Warner, K. L. Roinick, K. M. Arndt, Rtf1 is a multifunctional component of the Paf1 complex that regulates gene expression by directing cotranscriptional histone modification. *Mol. Cell. Biol.* **27**, 6103–6115 (2007).
51. A. Perez-Riba, L. S. Itzhaki, The tetratricopeptide-repeat motif is a versatile platform that enables diverse modes of molecular recognition. *Curr. Opin. Struct. Biol.* **54**, 43–49 (2019).
52. C. G. Amrich *et al*., Cdc73 subunit of Paf1 complex contains C-terminal Ras-like domain that promotes association of Paf1 complex with chromatin. *J. Biol. Chem.* **287**, 10863–10875 (2012).
53. M. A. Hahn *et al*., The tumor suppressor CDC73 interacts with the ring finger proteins RNF20 and RNF40 and is required for the maintenance of histone 2B monoubiquitination. *Hum. Mol. Genet.* **21**, 559–568 (2012).
54. A. D. Wier, M. K. Mayekar, A. Héroux, K. M. Arndt, A. P. VanDemark, Structural basis for Spt5-mediated recruitment of the Paf1 complex to chromatin. *Proc. Natl. Acad. Sci. U.S.A.* **110**, 17290–17295 (2013).
55. T. Xiao *et al*., Histone H2B ubiquitylation is associated with elongating RNA polymerase II. *Mol. Cell. Biol.* **25**, 637–651 (2005).
56. Y. Xu *et al*., Architecture of the RNA polymerase II-Paf1C-TFIIS transcription elongation complex. *Nat. Commun.* **8**, 15741 (2017).
57. P. Kumar *et al*., Role of a non-canonical surface of Rad6 in ubiquitin conjugating activity. *Nucleic Acids Res.* **43**, 9039–9050 (2015).
58. B. L. Hanson, C. Alexander, J. M. Harp, G. J. Bunick, Preparation and crystallization of nucleosome core particle. *Methods Enzymol.* **375**, 44–62 (2004).